Published OnlineFirst July 3, 2015; DOI: 10.1158/1535-7163.MCT-15-0129

protein varied according to SN38 timing with statistical significance in clock-proficient Caco-2 cells (ANOVA, $P < 0.0001$; Fig. 4A). Indeed, mean DNA-bound TOP1 amount nearly doubled between treatment at T2 and T14 ($P = 0.011$) or T20 ($P = 0.02$), whereas differences between T14 and T20 were minor and not statistically significant (ANOVA, $P = 0.86$). In contrast, DNA-bound TOP1 protein amount did not differ according to SN38 timing in clock-defective cells, with amounts similar to those found in clock-proficient cells treated at T2.

Circadian variations of irinotecan-induced apoptosis

The implications of the circadian clock control of molecular chronoPK and chronoPD for drug toxicity was further determined, through the quantification of caspase-3 activation as a marker of drug-induced apoptosis. Clock-proficient cells exposed to control siRNA displayed statistically significant time-dependent apoptosis (ANOVA, $P < 0.0001$; Fig. 4B). Apoptosis induction was increased by 14%, 52%, and 63% following irinotecan treatment at T2, T14, and T20, respectively, as compared with untreated controls. We thus observed a 4.5-fold difference in irinotecan-induced apoptosis as a function of whether irinotecan treatment was initiated at T2 or T20.

Modest time-dependent changes were found according to irinotecan timing in clock-defective cells. No statistically significant difference characterized treatment initiated at T2 or T14 ($P = 0.38$), yet apoptosis induction was largest at T20 as compared with T14 ($P = 0.002$) or T2 ($P = 0.025$). Clock silencing with *BMAL1* siRNA dramatically decreased irinotecan-induced apoptosis by 72% in cells treated at T14 and by 65% in cells treated at T20. In contrast, apoptosis increased by 25% in the siBMAL1 Caco-2 cells treated at T2 as compared with control conditions.

Model-based analysis of irinotecan chronoPK–PD

A comprehensive mathematical analysis of all the above experimental results was implemented. We first fitted the mathematical model of irinotecan molecular chronoPK–PD to the current multidimensional datasets (see Materials and Methods and Supplementary Data). In the presence of *BMAL1* siRNA treatment, all circadian rhythms were assumed to be disrupted—that is all circadian amplitudes were set to zero—and mean protein activities were allowed to be different from control conditions as suggested by differences in the mean mRNA levels of metabolism genes.

The calibrated mathematical model displayed good qualitative and quantitative agreement with all datasets, thus theoretically confirming the circadian disruption through *BMAL1* siRNA (Figs. 3 and 4). The Pearson χ^2 test validated, with a probability $P > 0.975$, that the irinotecan PK–PD model was correctly representing the 3 datasets of irinotecan PK, TOP1 activity, and drug-induced apoptosis measured at T2, T14, and T20 in both control and siBMAL1-exposed cells. The model predicted circadian activities for the proteins involved in irinotecan bioactivation (CES), SN38 detoxification (UGT1As), as well as for those responsible for irinotecan and SN38 efflux (ABC_CPT, ABC_SN) in control conditions. Predicted amplitude values (A^{activity}) ranged from 12.7% to 80% of the corresponding mean values (M^{activity}) and predicted acrophases ($\varphi^{\text{activity}}$) were shifted by 2 h 08 to 20 h 30 as compared with those of the corresponding mRNA expression rhythms (Fig. 5A and Supplementary Table S2). Furthermore, the fitting procedure predicted a circadian rhythm in k_{apop}, the parameter that links drug-induced DNA damage to apoptosis in the model. This finding suggested an important impact of the circadian control of DNA repair and apoptosis genes and proteins for irinotecan cytotoxicity. The best-fit model predicted highest cytotoxicity following drug exposure onset at 17 h 48 min and least if drug exposure timing started at 5 h 24 min modulo the period of 28 h 06 min (Fig. 4C).

In cells exposed to *BMAL1* siRNA, mean activities of irinotecan efflux transporters and UGT1As enzymes were unchanged compared with clock-proficient cells. In contrast, SN38 efflux transporters and irinotecan bioactivation activities were decreased by 17% and 37%, respectively. The k_{apop} model parameter value was increased by 2.85-fold compared with control, a result supporting a greater susceptibility of clock-deficient cells to irinotecan-induced DNA damage (Supplementary Table S2). The comprehensive mathematical model was consistent with all experimental data except the time-dependent changes in irinotecan extracellular concentrations in the clock-proficient cells, which were not well reproduced by the best-fit simulations. An additional *in vitro* chronoPK experiment was thus performed (See Supplementary Fig. S2). Overall, interstudy variability was considered as accounting for the minor discrepancy in irinotecan extracellular dynamics between both experiments.

The influence of model parameters on irinotecan toxicity pattern was assessed through global sensitivity analyses using DNA damage as the main toxicity endpoint (see Materials and Methods). Parameter sensitivity analyses were performed for (i) the circadian timing of irinotecan exposure onset associated to minimal DNA damage and (ii) the circadian amplitude of irinotecan-induced DNA damage, defined as the difference between the mean and the minimum values of the rhythm.

The circadian timing corresponding to least toxicity was mostly determined by the mean value and the circadian amplitude of both SN38 detoxification (UGT1A) and irinotecan bioactivation (CES), whose respective circadian acrophases ranked as first and second most sensitive parameters (Figs. 5B and 6). Irinotecan exposure duration ranked third, and the detoxification and bioactivation circadian amplitudes ranked fourth and fifth, respectively.

The amplitude of the toxicity rhythm was largely determined by the 3 circadian parameters of bioactivation, whose amplitude, mean value, and acrophase ranked as first, second, and fifth most sensitive parameters, respectively (Figs. 5C and 6). DNA complex formation and dissociation parameters also contributed to drug toxicity amplitude as k_{f1} (DNA/TOP1 complex formation), k_{f2} (SN38/DNA/TOP1 complex formation), k_{d1} (DNA/TOP1 complex dissociation), k_{DSB} (irreversible complex formation), and k_{d2} (SN38/DNA/TOP1 complex dissociation), respectively, ranked as third, sixth, seventh, eighth, and ninth parameters.

Discussion

Improving our understanding of the circadian rhythms that govern anticancer drug toxicities and efficacy requires identifying the critical molecular determinants of the circadian control of drug metabolism. To this end, we here investigated the *in vitro* chronopharmacology of irinotecan as a first proof of concept of chronopharmacology in synchronized cancer cell populations. This novel *in vitro–in silico* approach to

Published OnlineFirst July 3, 2015; DOI: 10.1158/1535-7163.MCT-15-0129

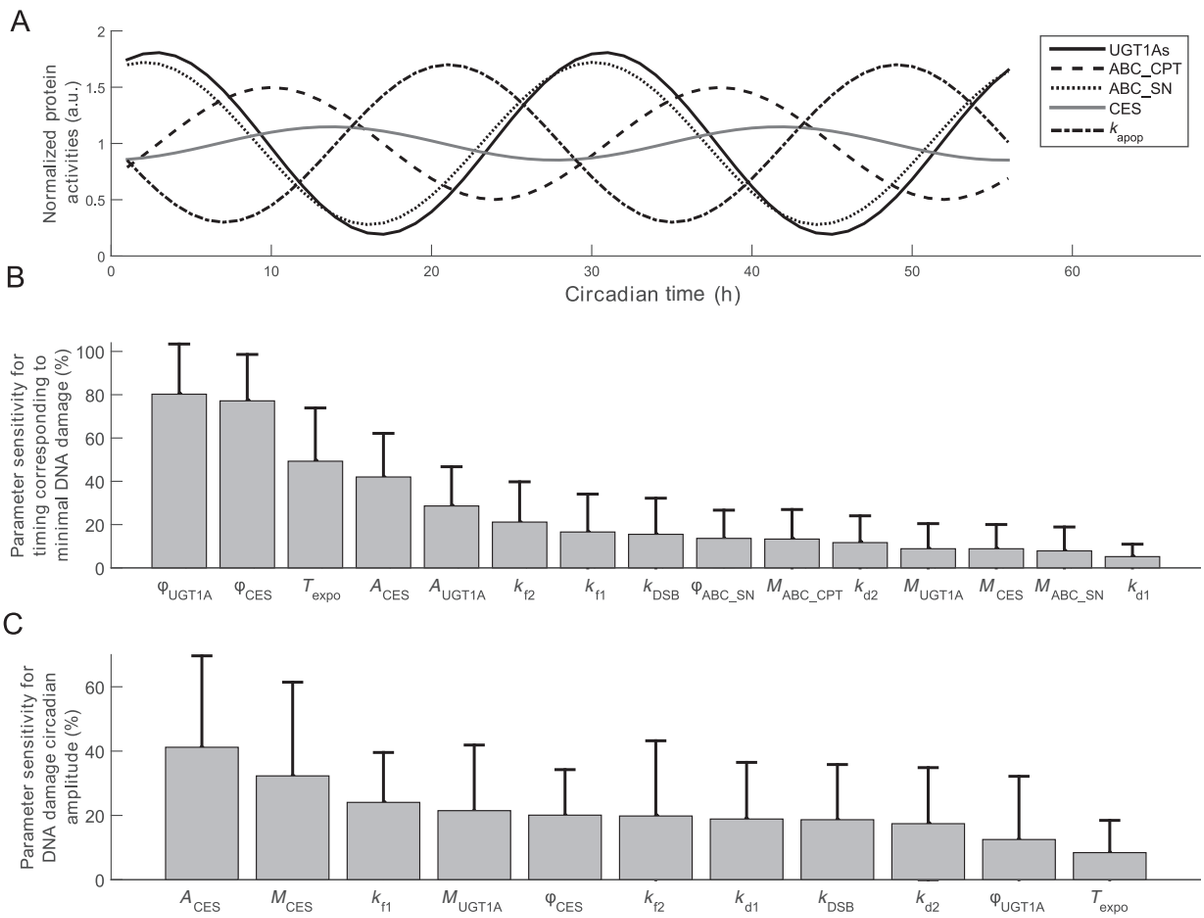

Figure 5.
Model-based predictions of molecular determinants of irinotecan cytotoxicity circadian pattern. A, protein activity circadian rhythms in control cells regarding irinotecan bioactivation (CES), irinotecan efflux (ABC_CPT), SN38 efflux (ABC_SN), SN38 detoxification (UGT1As), and the DNA damage phenotype (k_{apop}). B, parameter sensitivity for irinotecan circadian timing resulting in minimal DNA damage. The circadian phase (φ) of SN38 detoxification (UGT1As) and irinotecan bioactivation (CES) ranked as first and second most sensitive parameters. Their total-order sensitivity indices—that is, the contribution of the corresponding parameter to the change obtained in the minimal toxicity timing when all parameters are varied over their entire range—were equal to 80.2% and 77.2%, respectively. Their circadian amplitudes (A) ranked as fourth and fifth parameters, with indices of 28.6% and 42%, respectively. Irinotecan exposure duration (T_{expo}) also largely influenced the circadian timing corresponding to least cytotoxicity, as its total-order sensitivity indices ranked third and reached 49.3%. C, parameter sensitivity for the amplitude of DNA damage rhythm. This output was largely influenced by the bioactivation genes whose rhythm amplitude (A), mean value (M), and acrophase (φ) ranked as first, second, and fifth most sensitive parameters, with respective indices equal to 41.2%, 32.3%, and 20.1%. Parameters involved in DNA complex formation and dissociation also played role, as k_{f1} (DNA/TOP1 complex formation), k_{f2} (SN38/DNA/TOP1 complex formation), k_{d1} (DNA/TOP1 complex dissociation), k_{DSB} (irreversible complex formation), and k_{d2} (SN38/DNA/TOP1 complex dissociation), respectively, ranked as third, sixth, seventh, eighth, and ninth parameters.

developmental chronotherapeutics should be viewed as aiming to help dissect the relative contribution of the cellular molecular clock and that of systemic factors for the chronopharmacology of irinotecan. Here, circadian rhythms in irinotecan pharmacology and toxicity were found for each studied parameter in synchronized Caco-2 cell cultures and were all ablated following exposure to *BMAL1* siRNA. Thus, irinotecan chronopharmacology resulted from the control of its metabolism by the molecular circadian clock. Moreover, irinotecan cytotoxicity appeared to be positively correlated to the expression level of clock gene *BMAL1*, both in clock-proficient and in clock-deficient cells. In contrast, the cytotoxicity of oxaliplatin, another effective anticancer drug against colorectal cancer, reportedly displayed a negative correlation with *BMAL1* expression level (33). Taken together, the findings suggest that *BMAL1* tumor expression could help select the most effective drug for a given patient.

The physiologically based model of irinotecan chronoPK–PD closely agreed with experimental results. Model parameter sensitivity analyses highlighted the overall predominant influence of bioactivating CES and detoxifying UGT1As circadian rhythms on irinotecan chronotoxicity pattern. The mRNA expression circadian rhythms were in good agreement with previously published data (24). The circadian acrophases of *BMAL1*, *TOP1*, *UGT1A1*. and *ABCB1* were indeed similar to those earlier found in a separate study, whereas those of *PER2*, *REV-ERBα* and *CES2* differed by less than $\frac{\pi}{2}$ rad (Supplementary Fig. S3). The mathematical model of irinotecan chronoPK–PD, which was initially designed

Published OnlineFirst July 3, 2015; DOI: 10.1158/1535-7163.MCT-15-0129

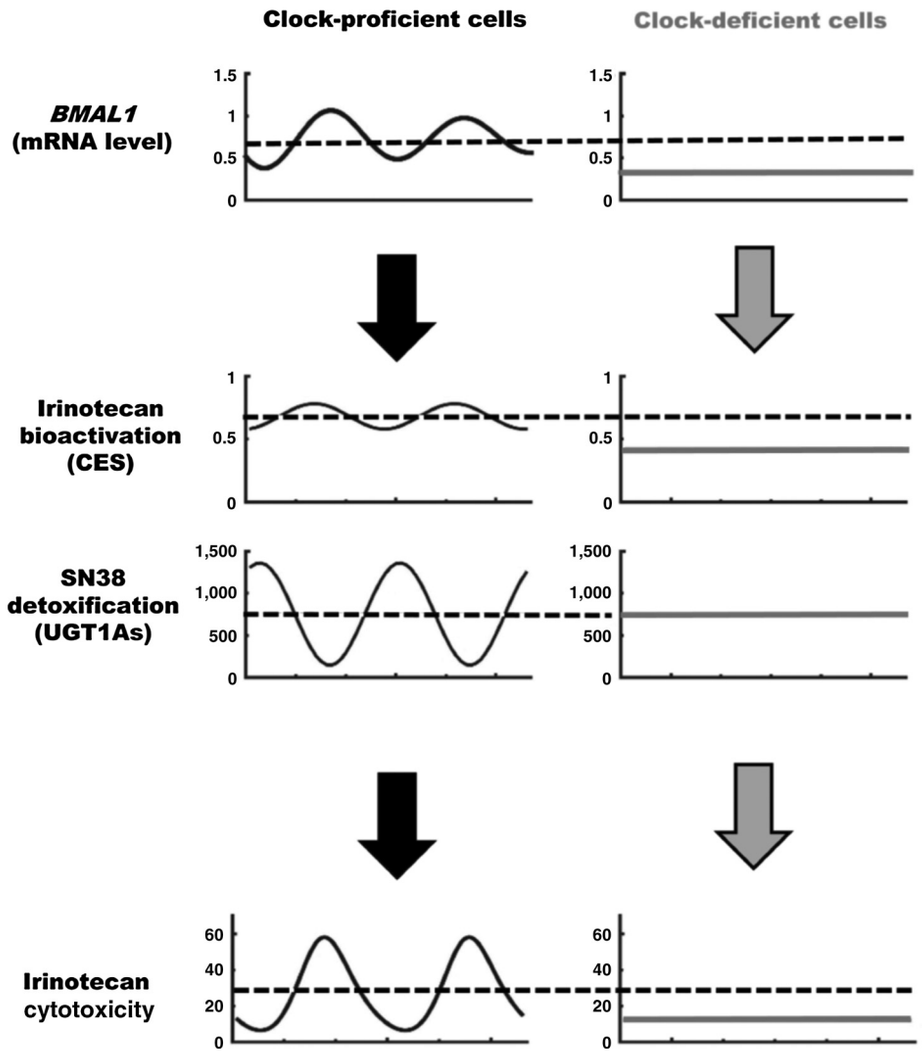

Figure 6.
Scheme summarizing the main molecular determinants of irinotecan cytotoxicity according to clock proficiency (left column) or clock deficiency (right column). Clock-proficient cells display a rhythmic *BMAL1* mRNA expression (first row), which regulates irinotecan bioactivation through CES activities (second row) and SN38 detoxification through UGT1A activities (third row), resulting in circadian pattern in irinotecan cytotoxicity (fourth row). Clock-deficient cells display flat patterns for all the parameters. The mean value of irinotecan bioactivation is reduced as compared with clock-proficient cells, which results in low cytotoxicity. Note the tight temporal coordination of bioactivation and detoxification in clock-proficient cells. The positive relation between *BMAL1* mRNA expression and irinotecan cytotoxicity both in clock-proficient and in clock-deficient cells supports the potential relevance of *BMAL1* as a predictive biomarker of irinotecan cytotoxicity.

for unsynchronized Caco-2 cells, successfully fitted the current datasets in synchronized cells, a step that further validated the model structure. New parameter estimates were obtained here, which highlighted kinetics differences between synchronized and unsynchronized cells, thus providing an opportunity for differentiating chronopharmacology in healthy and malignant tissues (Supplementary Table S3).

An interesting added value of the model involved its ability to accurately predict the circadian patterns in the main metabolism proteins, based upon gene and pharmacology data. The estimated protein acrophases were shifted by 1 h 24 min to 20 h 30 min relative to those found for the corresponding genes. Intervals ranging from 0 to 20 hours (modulo, 24 hours) were previously reported between several mRNA and protein expressions in mouse tissues (30). The model predictions based on synchronized Caco-2 data were rather consistent with mouse liver data, following the normalization of the circadian period to 24 hours for the Caco-2 cells. Thus, the model predicted a time lag of 14 hours for UGT1As mRNA and protein expression rhythms, whereas it was equal to 15 hours for *Ugt1a1* in mouse liver (30). Similarly, the model predicted a 22-hour time lag between CES mRNA and protein, which differed from mouse liver *Ces2* by only 4 hours (30).

The slight shift between the circadian rhythm in irinotecan-induced DNA-bound TOP1 and that in extent of apoptosis suggested the occurrence of an additional circadian control of DNA repair and apoptosis processes. The best-fit mathematical model indeed included a non-zero circadian amplitude for the parameter k_{apop}, which represents the DNA damage response phenotype, including the *P53* network, DNA repair and, eventually, apoptosis. Besides its regulatory effect on apoptosis, *P53* also regulates the molecular clock so that *P53* mutation could modify the circadian rhythms of the protein activities involved in irinotecan chronopharmacology and therefore alter the circadian pattern in irinotecan cytotoxicity (29, 34).

Altogether, the current model-driven chronopharmacology study has established the molecular bases of irinotecan chronopharmacology, through setting up a comprehensive

mechanistic circadian PK–PD model for this drug. Several levels of prediction have been confirmed, regarding the circadian control of gene transcription and proteins, based on a recent literature survey. Moreover, the temporal relation between low *BMAL1* expression and low irinotecan toxicity found *in vitro* was in good agreement with experimental studies in mice regarding the circadian toxicity pattern of this drug as well (23). The results advocate thus for the model validity and accuracy, which now deserves further prospective adjustments in selected experimental models, before clinical testing of personalized chronopharmacology delivery in cancer patients.

Disclosure of Potential Conflicts of Interest

No potential conflicts of interest were disclosed.

Authors' Contributions

Conception and design: S. Dulong, A. Ballesta, A. Okyar, F. Lévi
Development of methodology: S. Dulong, A. Ballesta, F. Lévi
Acquisition of data (provided animals, acquired and managed patients, provided facilities, etc.): S. Dulong, F. Lévi
Analysis and interpretation of data (e.g., statistical analysis, biostatistics, computational analysis): S. Dulong, A. Ballesta, A. Okyar, F. Lévi
Writing, review, and/or revision of the manuscript: S. Dulong, A. Ballesta, A. Okyar, F. Lévi
Administrative, technical, or material support (i.e., reporting or organizing data, constructing databases): S. Dulong, A. Ballesta
Study supervision: S. Dulong, A. Ballesta, F. Lévi

Acknowledgments

The authors thank Dr. Jean Clairambault for his role in the initiation of this project and subsequent fruitful discussions.

Grant Support

This work was co-funded by the ARC (CR109/8003) to F. Lévi, the European Commission through the specific targeted research project TEMPO (*LSHG-CT-2006-037543*) to all authors, *ERASysBio+ (C5Sys, LHSB-2010-005137)* to F. Lévi and S. Dulong, CaSyM (HEALTH-F4-2012-305033) to A. Ballesta and F. Lévi, and the research fund of Istanbul University (N-7762/2010) to A. Okyar.

The costs of publication of this article were defrayed in part by the payment of page charges. This article must therefore be hereby marked *advertisement* in accordance with 18 U.S.C. Section 1734 solely to indicate this fact.

Received February 11, 2015; revised May 18, 2015; accepted June 23, 2015; published OnlineFirst July 3, 2015.

References

1. Dibner C, Schibler U, Albrecht U. The mammalian circadian timing system: organization and coordination of central and peripheral clocks. Annu Rev Physiol 2010;72:517–49.
2. Levi F, Okyar A, Dulong S, Innominato PF, Clairambault J. Circadian timing in cancer treatments. Annu Rev Pharmacol Toxicol 2010;50:377–421.
3. Levi F, Schibler U. Circadian rhythms: mechanisms and therapeutic implications. Annu Rev Pharmacol Toxicol 2007;47:593–628.
4. Ortiz-Tudela E, Mteyrek A, Ballesta A, Innominato PF, Levi F. Cancer chronotherapeutics: experimental, theoretical, and clinical aspects. Handb Exp Pharmacol 2013:261–88.
5. Innominato PF, Giacchetti S, Bjarnason GA, Focan C, Garufi C, Coudert B, et al. Prediction of overall survival through circadian rest-activity monitoring during chemotherapy for metastatic colorectal cancer. Int J Cancer 2012;131:2684–92.
6. Innominato PF, Giacchetti S, Moreau T, Bjarnason GA, Smaaland R, Focan C, et al. Fatigue and weight loss predict survival on circadian chemotherapy for metastatic colorectal cancer. Cancer 2013;119:2564–73.
7. Innominato PF, Roche VP, Palesh OG, Ulusakarya A, Spiegel D, Levi FA. The circadian timing system in clinical oncology. Ann Med 2014;46:191–207.
8. Mormont MC, Levi F. Circadian-system alterations during cancer processes: a review. Int J Cancer 1997;70:241–7.
9. Ortiz-Tudela E, Iurisci I, Beau J, Karaboue A, Moreau T, Rol MA, et al. The circadian rest-activity rhythm, a potential safety pharmacology endpoint of cancer chemotherapy. Int J Cancer 2014;134:2717–25.
10. Roche VP, Mohamad-Djafari A, Innominato PF, Karaboue A, Gorbach A, Levi FA. Thoracic surface temperature rhythms as circadian biomarkers for cancer chronotherapy. Chronobiol Int 2014;31:409–20.
11. Gachon F, Olela FF, Schaad O, Descombes P, Schibler U. The circadian PAR-domain basic leucine zipper transcription factors DBP, TEF, and HLF modulate basal and inducible xenobiotic detoxification. Cell Metab 2006;4:25–36.
12. Panda S, Antoch MP, Miller BH, Su AI, Schook AB, Straume M, et al. Coordinated transcription of key pathways in the mouse by the circadian clock. Cell 2002;109:307–20.
13. Eckel-Mahan KL, Patel VR, Mohney RP, Vignola KS, Baldi P, Sassone-Corsi P. Coordination of the transcriptome and metabolome by the circadian clock. Proc Natl Acad Sci U S A 2012;109:5541–6.
14. Fustin JM, Doi M, Yamada H, Komatsu R, Shimba S, Okamura H. Rhythmic nucleotide synthesis in the liver: temporal segregation of metabolites. Cell Rep 2012;1:341–9.
15. Pommier Y. Topoisomerase I inhibitors: camptothecins and beyond. Nat Rev Cancer 2006;6:789–802.
16. Gilbert DC, Chalmers AJ, El-Khamisy SF. Topoisomerase I inhibition in colorectal cancer: biomarkers and therapeutic targets. Br J Cancer 2012;106:18–24.
17. Ahowesso C. Approche expérimentale de la personnalisation de la chronothérapeutique par irinotecan. Université Paris 2011.
18. Kuramoto Y, Hata K, Koyanagi S, Ohdo S, Shimeno H, Soeda S. Circadian regulation of mouse topoisomerase I gene expression by glucocorticoid hormones. Biochem Pharmacol 2006;71:1155–61.
19. Ahowesso C, Li XM, Zampera S, Peteri-Brunback B, Dulong S, Beau J, et al. Sex and dosing-time dependencies in irinotecan-induced circadian disruption. Chronobiol Int 2011;28:458–70.
20. Ando H, Yanagihara H, Sugimoto K, Hayashi Y, Tsuruoka S, Takamura T, et al. Daily rhythms of P-glycoprotein expression in mice. Chronobiol Int 2005;22:655–65.
21. Okyar A, Piccolo E, Ahowesso C, Filipski E, Hossard V, Guettier C, et al. Strain- and sex-dependent circadian changes in abcc2 transporter expression: implications for irinotecan chronotolerance in mouse ileum. PLoS One 2011;6:e20393.
22. Filipski E, Berland E, Ozturk N, Guettier C, van der Horst GT, Levi F, et al. Optimization of irinotecan chronotherapy with P-glycoprotein inhibition. Toxicol Appl Pharmacol 2014;274:471–9.
23. Li XM, Mohammad-Djafari A, Dumitru M, Dulong S, Filipski E, Siffroi-Fernandez S, et al. A circadian clock transcription model for the personalization of cancer chronotherapy. Cancer Res 2013;73:7176–88.
24. Ballesta A, Dulong S, Abbara C, Cohen B, Okyar A, Clairambault J, et al. A combined experimental and mathematical approach for molecular-based optimization of irinotecan circadian delivery. PLoS Comput Biol 2011;7:e1002143.
25. Goldwasser F, Bae I, Valenti M, Torres K, Pommier Y. Topoisomerase I-related parameters and camptothecin activity in the colon carcinoma cell lines from the National Cancer Institute anticancer screen. Cancer Res 1995;55:2116–21.

Published OnlineFirst July 3, 2015; DOI: 10.1158/1535-7163.MCT-15-0129

26. Subramanian D, Kraut E, Staubus A, Young DC, Muller MT. Analysis of topoisomerase I/DNA complexes in patients administered topotecan. Cancer Res 1995;55:2097–103.
27. Chomczynski P, Sacchi N. Single-step method of RNA isolation by acid guanidinium thiocyanate-phenol-chloroform extraction. Anal Biochem 1987;162:156–9.
28. Teboul M, Delaunay F. [No hierarchy in mammalian circadian system]. Med Sci (Paris) 2004;20:628–9.
29. Sancar A, Lindsey-Boltz LA, Kang TH, Reardon JT, Lee JH, Ozturk N. Circadian clock control of the cellular response to DNA damage. FEBS Lett 2010;584:2618–25.
30. Mauvoisin D, Wang J, Jouffe C, Martin E, Atger F, Waridel P, et al. Circadian clock-dependent and -independent rhythmic proteomes implement distinct diurnal functions in mouse liver. Proc Natl Acad Sci U S A 2014;111:167–72.
31. Schwanhausser B, Busse D, Li N, Dittmar G, Schuchhardt J, Wolf J, et al. Global quantification of mammalian gene expression control. Nature 2011;473:337–42.
32. Saltelli A, Ratto M, Andres T, Campolongo F, Cariboni J, Gatelli D, et al. Global sensitivity analysis. The primer. Chichester, England: Wiley; 2008.
33. Zeng ZL, Luo HY, Yang J, Wu WJ, Chen DL, Huang P, et al. Overexpression of the circadian clock gene Bmal1 increases sensitivity to oxaliplatin in colorectal cancer. Clin Cancer Res 2014;20:1042–52.
34. Miki T, Matsumoto T, Zhao Z, Lee CC. p53 regulates Period2 expression and the circadian clock. Nat Commun 2013;4:2444.